

EFFECT OF DIFFUSION ON $(\text{ZrO}_2)_{0.8}(\text{Y}_2\text{O}_3)_{0.2}$ CERAMIC

S.V. SHARMA AND P. CHAND

Department of Physics, Indian Institute of Technology, Kanpur 208 016 (UP), India

(Received February 14, 1995)

Effect of iodine and lithium diffusion on undoped and doped (with transition metal ions: Ti, V, Ni, Fe, Cu, Co and Mn) samples of polycrystalline $(\text{ZrO}_2)_{0.8}(\text{Y}_2\text{O}_3)_{0.2}$ ceramic has been investigated using X-ray diffraction, scanning electron microscopy and electron paramagnetic resonance.

PACS numbers: 61.16.-d, 64.80.Gd, 66.30.-h, 76.30.Fc, 81.20.Lb

1. Introduction

The ever increasing application of the zirconia (ZrO_2) ceramic, in high technology particularly in wear parts and as solid electrolytes, has attracted a great deal of attention [1-7]. There are three known polymorphs of ZrO_2 namely, monoclinic (M), tetragonal (T) and cubic (C) [5]. The effect of Nb_2O_5 alloying on thermal expansion anisotropy of 2 mol% yttria stabilized tetragonal zirconia has been studied by Kim et al. [8]. Diffusionless tetragonal to cubic transformation in zirconia-ceria solid solutions has been reported by Yashima et al. [9]. Lithium (Li) diffusion is expected to take place easily in the solid electrolytes and the diffusion can remarkably change the electrical conductivity of the solids [10]. It is also of interest to study the microstructure which develops during the sintering/diffusion. EPR is a sensitive technique to provide information about the valence state and the local environment of the probe ion. The structural information obtained from X-ray diffraction (XRD) and scanning electron microscopy (SEM) can be correlated with the results of electron paramagnetic resonance (EPR) studies to gather more understanding regarding the microstructural and other properties of the ceramics. Keeping this in view we have doped the zirconia-yttria ceramic with different 3d transition metal ions. In a previous communication [11] we have reported the results of EPR and structural studies of pure and doped (with Fe, Ni, Co, and V) $(\text{ZrO}_2)_{0.8}(\text{Y}_2\text{O}_3)_{0.2}$ ceramics. In the present investigations similar studies have been extended to the Ti, Cu and Mn doped samples of $(\text{ZrO}_2)_{0.8}(\text{Y}_2\text{O}_3)_{0.2}$. The effect of exposure to iodine (I_2) and Li vapours on pure and doped with transition metal ions Ti, V, Cu, Mn, Fe, Ni or Co $(\text{ZrO}_2)_{0.8}(\text{Y}_2\text{O}_3)_{0.2}$ ceramic samples

are studied with the help of EPR in addition to the structural studies. Iodine is used as a complementary dopant to Li. The results obtained from these studies are presented and discussed here.

2. Experimental

The details of synthesis of the samples have been reported elsewhere [11]. The transition metal impurities were taken from $\text{Cu}(\text{NO}_3)_2 \cdot 3\text{H}_2\text{O}$ for Cu, $\text{MnCl}_2 \cdot 4\text{H}_2\text{O}$ for Mn and TiO_2 for Ti for the purpose of doping. The samples are coded according to the doped impurities for example SZYMn represents the $(\text{ZrO}_2)_{0.8}(\text{Y}_2\text{O}_3)_{0.2}$ sample doped with manganese impurity. Exposure to Li vapours was carried out at 1650 K for half an hour duration. The samples were exposed to iodine vapours for various durations (1 h to 12 days) and at various temperatures between 300 K and 773 K to see the effects of exposure.

The XRD patterns were recorded using a Rich Seifert Isodebyeflex 2002 diffractometer with $\text{Cu } K_\alpha$ radiation. The SEM micrographs were taken on a JEOL SEM at a fixed magnification of 5000 at 15 kV. EPR measurements were done with the help of an X-band EPR spectrometer (Varian E-109) using 100 kHz phase sensitive detection.

3. Results and discussion

XRD study of the samples revealed the presence of all the three known phases M, T and C of the ceramic. The concentrations of the phases in the samples were estimated as reported earlier [11, 12] and the values are given in Table I. From this table we can infer that in all the samples the M phase is the dominant phase. The XRD studies of exposed (either to Li or to I_2) samples do not show discernible changes in the XRD patterns. Consequently, we could not estimate any changes in the phase composition of the samples after exposures.

TABLE I
The relative phase composition of the three phases: M, T and C.

Sample No.	Sample	Relative concentration of phases (%)		
		M	T	C
1	SZYP	61	33	6
2	SZYT _i	58	33	9
3	SZ _Y V	65	30	5
4	SZ _Y M _n	63	32	5
5	SZ _Y Fe	61	33	6
6	SZ _Y N _i	63	32	5
7	SZ _Y Co	62	33	5
8	SZ _Y Cu	62	32	6

The SEM micrographs of the samples show different kinds of microstructure. The average grain size varies from sample to sample. The grain size estimates obtained from the SEM micrographs indicate broadly two ranges of particle-size: larger grains ($> 5 \mu\text{m}$) and smaller grains ($< 1 \mu\text{m}$). Generally, sintering temperature and duration, preparation methods, etc., are the parameters which critically affect the microstructure of the final product. Since we have followed a fixed heat treatment for sintering to all the samples, the variation in average grain size in this case may be attributed largely to the effect of dopants. After exposing the samples to Li vapours, the SEM micrographs show only marginal changes in the microstructure except for the samples SZYCu and SZYMn which show striking changes in the microstructural features (Fig. 1).

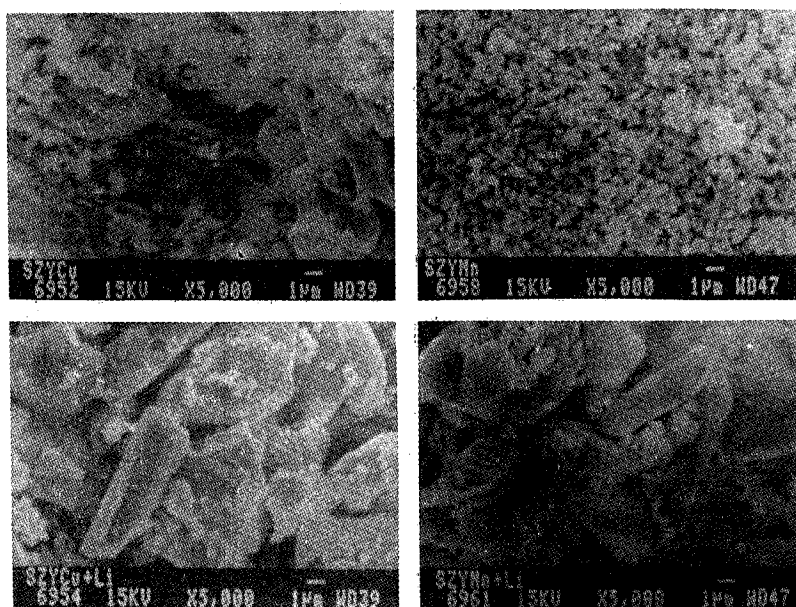


Fig. 1. Typical SEM micrographs of SZYCu and SZYMn before and after exposure to Li vapours.

The EPR spectra of the powdered (finely crushed) undoped samples (SZYP), vanadium doped (SZYV), nickel doped (SZYNi), iron doped (SZYFe), and cobalt doped (SZYCo) were reported earlier [11]. The interesting aspect of the EPR signals of SZYP is that their widths and positions remain essentially temperature independent between room temperature (RT) and liquid nitrogen temperature (LNT) and no discernible changes occur in the EPR spectrum even after prolonged exposures to I_2 or Li vapours. It is interesting to mention here that iodine exposures for durations up to 12 days and at temperatures up to 773 K are found to be ineffective to produce any discernible changes in the EPR of doped samples too.

The EPR spectrum of titanium doped sample SZYTi comprises a large number of narrow lines in addition to the two signals observed in SZYP [11]. Diver-

lent titanium complexes are very unstable, however, trivalent titanium with electronic configuration $[Ar]3d^1$ forms stable octahedral paramagnetic complexes and EPR can be observed at RT/LNT with g -factor smaller than free electronic value $g_e (= 2.0023)$. Hyperfine splittings may occur due to ^{47}Ti and ^{49}Ti isotopes [13]. The observed EPR spectrum in the present case is not appropriate to any of the above two paramagnetic states of titanium. The large number of narrow lines on the broad signal (the so-called grass structure) is too complex to be analyzed meaningfully. Also no discernible changes occur in the EPR spectrum after exposure to either Li or I_2 vapours.

EPR spectrum of vanadium doped sample SZYV has been discussed earlier [11]. After exposure to Li vapours, the intensity of EPR signal decreases significantly retaining the other features. This indicates the conversion of the vanadium impurity from paramagnetic to diamagnetic form on exposure.

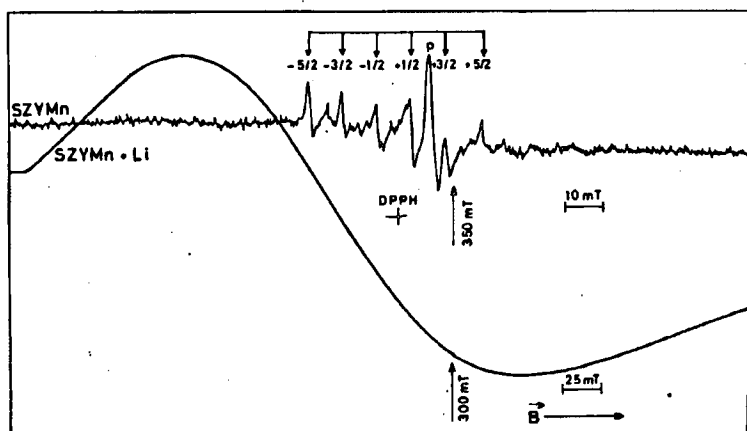


Fig. 2. X-band EPR spectra of SZYMn and Li exposed sample SZYMn+Li at RT. Standard DPPH g -marker is shown. The intrinsic signal is marked by p . p is obscured in Li-exposed sample.

The EPR spectra of SZYMn are shown in Fig. 2. In addition to the two characteristic signals of the undoped sample other signals are also observed which are characteristic signals of Mn^{2+} ion in a crystalline field of cubic symmetry [13]. Usually a thirty line spectrum is expected for Mn^{2+} in a crystal [12–15], however, in cubic environment a six line spectrum may result due to overlapping of fine structure transitions. The isotropic EPR parameters (g_0 and $|A_0|$) obtained from the analysis of the spectrum are collated in Table II. It is interesting to compare these results with those reported by Stempi et al. [16] for manganese doped single crystals of $(\text{ZrO}_2)_{0.8}(\text{Y}_2\text{O}_3)_{0.2}$. They have observed a six line spectrum at $g \approx 2$ with hyperfine parameter $|A| \approx 8.3$ mT ($1 \text{ mT} = 10^{-3} \text{ tesla} = 10 \text{ gauss}$) as compared to $|A| = 9.4$ mT in the present case and attributed it to Mn^{2+} ion substituting either Zr^{4+} or Y^{3+} ions at lattice sites such that a trigonal distortion occurs due to charge compensation requirements. The magnitude of hyperfine interaction parameter $|A|$ may provide a measure of covalency of metal ion. It is

TABLE II
EPR parameters of unexposed samples.

Sample	g value	Hyperfine parameters A [mT]*	Linewidth ΔH [mT]
SZYTi	$g_p = 1.975 \pm 0.005$	$A_0 = 9.4$	2.5 ± 0.3
	$g_a = 3.736 \pm 0.005$		169 ± 5
SZYMn	$g_p = 1.975 \pm 0.005$		2.5 ± 0.3
	$g_0 = 2.031 \pm 0.005$		2.0 ± 0.3
SZYFe	$g_p = 1.975 \pm 0.005$		2.5 ± 0.3
	$g_a = 2.184 \pm 0.005$		52 ± 5
	$g_b = 1.980 \pm 0.005$		25 ± 2
	$g_c = 1.881 \pm 0.005$		—
SZYNi	$g_p = 1.975 \pm 0.005$		2.5 ± 0.3
	$g_a = 2.544 \pm 0.005$		135 ± 5
SZYCu	$g_p = 1.975 \pm 0.005$	2.2 ± 0.3	
	$g_{\parallel} = 2.175 \pm 0.005$	$A_{\parallel} = 5.6$	—
	$g_{\perp} = 2.037 \pm 0.005$	$A_{\perp} = 2.4$	—

* To convert gauss into cm^{-1} multiply by $(g\mu_B/hc)$.

believed that $|A|$ decreases with covalency and a relation in $|A|$ and covalency has been established for Mn^{2+} in simple crystal systems by Šimánek and Müller [17]. Kiggins and Manooogian [18] computed the average value of $|A|$ for a number of complicated crystal systems, where Mn^{2+} is coordinated octahedrally to oxygen and found that for normal octahedral bonding the representative covalency parameter is about 7%. Significant deviations from this value would suggest a more complicated bonding of the metal ion with the surrounding atoms. The covalency parameter obtained with the help of reference [17] in our case is 7.5% and suggests a normal bonding of Mn^{2+} ion in octahedral oxygen environment.

Drastic changes in the EPR spectrum of sample SZYMn occur after exposing it to the Li vapours (Fig. 2). The most striking feature is the anomalous broadening of EPR signal and subsequent conversion of six line spectrum into a broad line signal after exposure. The changes in the EPR spectra imply segregation and a chemical change involving the manganese ions on exposure which are responsible for the broadening of the EPR signals. The values of peak to peak linewidth (ΔH) and g are given in Tables II and III along with the other EPR data.

The iron doped sample SZYFe shows a marginal broadening of the EPR signals after exposure retaining the other features. The broadening of EPR signal indicates a decrease in the relaxation time or a change in exchange interaction of the paramagnetic species. On the contrary, after exposure the nickel doped sample SZYNi shows a marginal reduction in linewidth of EPR signal as compared to the

TABLE III
EPR parameters of exposed (Li)
samples.

Sample code	g values	Linewidth ΔH [mT]
SZYTi	$g_p = 1.970$	2.5
	$g_a = 3.728$	170.0
SZYMn	$g = 3.164$	220.0
SZYFe	$g_p = 1.967$	2.5
	$g_a = 2.355$	152.5
SZYNi	$g_p = 1.966$	2.5
	$g_a = 2.527$	117.5
SZYCu	$g_p = 1.97$	2.5
	$g_a = 2.01$	*

* The signal is too broad and asymmetric.

unexposed sample. The narrowing of the signal implies an increase in relaxation time of Ni^{2+} ions due to Li diffusion in the sample. The parameters derived from the spectra are mentioned in Tables II and III. In contrast the cobalt doped sample does not show any EPR signals other than those of an undoped sample even after exposure and up to LNT.

The EPR spectrum of sample SZYCu is explained by the Cu^{2+} ($3d^9$) with $S = 1/2$ and $I = 3/2$. In the powdered sample one observes characteristic peaks corresponding to parallel (\parallel , i.e. $\theta = 0^\circ$) and perpendicular (\perp , i.e. $\theta = 90^\circ$) orientations similar to the case of VO^2 ions in axial symmetry [13, 19]. Here θ is the angle between the applied magnetic field and the tetragonal axis. The values of g_p , g_a , A_{\parallel} and A_{\perp} obtained from the analysis of the EPR spectra using expressions given in Ref. [20] are given in Table III. The most intriguing result observed in the Li exposed sample of SZYCu is that the signal becomes extremely broad and also asymmetric making the measurements of g and ΔH quite impossible. This observation is similar to the case of SZYMn. In this case also a chemical and exchange interaction change involving Cu^{2+} ions and segregation of the copper impurity complex is envisaged. It may be mentioned here that SEM has shown significant microstructural changes in samples SZYMn and SZYCu after exposure in conformity with the EPR results.

4. Conclusion

The EPR spectra of undoped sample SZYP do not display any discernible change on exposure to Li or I_2 . Only marginal changes are observed in the case of SZYTi, SZYNi, SZYFe and SZYV samples. The effect of exposure to lithium has been remarkably demonstrated in the case of samples SZYCu and SZYMn and

both EPR and SEM observations are in good accord to suggest microstructural changes. However, XRD is insensitive to these changes. Iodine exposure seems to be ineffective to cause any discernible changes in the EPR as well as structural studies. Therefore, LiI may be used for the purpose of Li diffusion in the zirconia based solid electrolytes.

References

- [1] R. Stevens, *Zirconia Engineering Ceramics, Handbook of Ceramics*, Suppl. to *Inter-ceram.* **34**, 1 (1985).
- [2] A.R. Burkin, H. Saricimen, B.C. Steel, *Trans. J. Brit. Ceram. Soc.* **79**, 105 (1980).
- [3] N.M. Ghoneim, S.B. Hanna, *J. Mater. Sci.* **25**, 5192 (1990).
- [4] N.R. Shankar, H. Herman, S.P. Singhal, C.C. Berndt, *Thin Solid Films* **119**, 159 (1984).
- [5] N. Iwamoto, N. Umesaki, S. Endo, *Thin Solid Films* **127**, 129 (1985).
- [6] R.A. Miller, J.L. Smialek, R.J. Garlick, *Adv. Ceramic* **3**, 241 (1981).
- [7] D. Michel, F. Faudot, E. Gaffet, L. Mazerolles, *J. Am. Ceram. Soc.* **76**, 2884 (1993).
- [8] D.J. Kim, P.F. Becher, C.R. Hubbard, *J. Am. Ceram. Soc.* **76**, 2904 (1993).
- [9] M. Yashima, K. Morimoto, N. Ishizawa, M. Yoshimura, *J. Am. Ceram. Soc.* **76**, 2865 (1993).
- [10] C.J. Chen, M. Greenblatt, *Mater. Res. Bull.* **20**, 1347 (1985).
- [11] B.N. Misra, S.V. Sharma, P. Chand, N.L. Shukla, *Phys. Status Solidi A* **139**, 295 (1993); N.L. Shukla, S.V. Sharma, P. Chand, B.N. Misra, *Acta Phys. Pol. A* **83**, 441 (1993).
- [12] B.D. Cullity, *Elements of X-ray Diffraction*, Addison-Wesley Publ. Comp. Inc., Menlo Park, California 1978.
- [13] J.E. Wertz, J.R. Bolton, *Electron Spin Resonance: Elementary Theory and Practical Applications*, McGraw Hill, 1972, Chap. 11.
- [14] A. Carrington, A.D. Mc Lachlan, *Introduction to Magnetic Resonance*, Chapman & Hall Ltd., New York 1979, Chap 10.
- [15] B. Bleaney, *Philos. Mag.* **42**, 441 (1951).
- [16] M. Stempi, H. Szymczak, A.A. Andreev, *Acta Phys. Pol. A* **63**, 627 (1983).
- [17] E. Šimánek, K.A. Müller, *J. Phys. Chem.* **31**, 1027 (1970).
- [18] B. Kiggins, A. Manoogian, *Cand. J. Phys.* **49**, 3174 (1971).
- [19] P. Chand, V.K. Jain, G.C. Upreti, *Magn. Reson. Rev.* **14**, 49 (1988).
- [20] A. Abragam, B. Bleaney, *Electron Paramagnetic Resonance of Transition Ions*, Clarendon Press, Oxford 1970.